



Contents lists available at ScienceDirect

Biochemical and Biophysical Research Communications

journal homepage: www.elsevier.com/locate/ybbrc

A novel bispecific nanobody with PD-L1/TIGIT dual immune checkpoint blockade

Linlin Ma ^{a,1}, Junwei Gai ^{b,1}, Peng Qiao ^{b,1}, Yanfei Li ^a, Xiaofei Li ^b, Min Zhu ^{b,***},
Guanghui Li ^{b,**}, Yakun Wan ^{b,*}

^a Shanghai Key Laboratory of Molecular Imaging, Shanghai University of Medicine and Health Sciences, Shanghai, China

^b Shanghai Novamab Biopharmaceuticals Co., Ltd., Shanghai, China

ARTICLE INFO

Article history:

Received 12 July 2020

Accepted 14 July 2020

Available online xxx

Keywords:

PD-L1

TIGIT

Nanobody

Bispecific antibody

ABSTRACT

Cancer immunotherapy have changed the paradigm of cancer treatment, but there remains a great need for improvement given that less patients with tumors respond to the treatment of PD-1/PD-L1 blockade. TIGIT (also called T cell immunoreceptor with Ig and ITIM domains), a novel immune checkpoint molecule, has been shown a promising target for drug development of immunotherapy. Here we report generation and characterization of a multivalent bispecific antibody (BsAb) that co-targets PD-L1 and TIGIT. The BsAb consists of tetravalent anti-PD-L1 Fc-fusion nanobody (Nb) and tetravalent anti-TIGIT Nb. The parental anti-PD-L1 Nb showed high specificity and affinity to primate PD-L1, the enhanced T cell activity *in vitro* and anti-tumor activity *in vivo*. Similarly, the parental anti-TIGIT Nb showed the high specificity and affinity to primate TIGIT and the enhanced T cell activity. Furthermore, we demonstrated that the BsAb retained high blocking activity towards PD-1/PD-L1 or TIGIT/CD155 interaction. The BsAb synergistically enhanced T cell activities *in vitro* compared to two parental Nbs. Taken together, we obtained a multivalent BsAb blocking biological function of PD-L1 and TIGIT and it is worthy to further study the anti-tumor activities of this BsAb *in vivo*.

© 2020 Elsevier Inc. All rights reserved.

1. Introduction

Cancer immunotherapy targeting immune checkpoint molecules, such as programmed cell death-1 (PD-1) and its ligand programmed death-ligand-1 (PD-L1), have changed the paradigm of cancer treatment, but there remains a great need for improvement, given that less than 50% of patients with tumors respond to the treatment of monoclonal antibodies (mAbs) targeting PD-1/PD-L1 [1,2]. Targeting other immune checkpoints including TIGIT (also called T cell immunoreceptor with Ig and ITIM domains) is a promising approach which might be synergistic with PD-1/PD-L1 mAbs in cancer treatment [3,4].

TIGIT is a novel immunoglobulin superfamily member expressed

majorly on T cells and NK cells [5]. Similar to other inhibitory checkpoints, TIGIT has been shown to play an important role in the response of antitumor immunity [6]. The protein delivers its immunosuppressive signals by binding to its ligand CD155 or CD112, resulting in the inhibition of T cell responses and NK cells cytotoxicity [7,8]. For instance, previous studies showed that TIGIT blockade or genetic ablation enhanced NK cell killing activities and CD8⁺ T cell effector function, reducing the tumor growth in multiple cancer models [4,9,10]. In contrast, administration of agonistic anti-TIGIT Abs demonstrated a direct inhibitory effect on NK cell and T cell function [11,12].

Considering that PD-1/PD-L1 enhances tumor immune evasion by exhausting CD8⁺ T cells, while TIGIT/CD155 achieves this at least partly by inhibiting NK cell killing, co-blockade of PD-1/PD-L1 and TIGIT/CD155 should theoretically have a synergistic anti-tumor effect. In fact, TIGIT and PD-1/PD-L1 dual blockades have been shown to synergistically inhibit tumor growth in the murine models of colorectal cancer and glioblastoma [13,14]. Recently, a TIGIT inhibitor tiragolumab combined with anti-PD-L1 mAb atezolizumab entered into a phase 2 trial (NCT03563716) for the treatment of locally advanced or metastatic non-small cell lung

* Corresponding author. Shanghai Novamab Biopharmaceuticals Co., Ltd., Room 201, No. 10, 500 FuRong Flower Road, Pudong New District, Shanghai, China.

** Corresponding author.

*** Corresponding author.

E-mail addresses: mzhu@novamab.com (M. Zhu), ghli@novamab.com (G. Li), ykwan@novamab.com (Y. Wan).

¹ These authors contribute equally.

Abbreviations

TIGIT	T cell immunoreceptor with Ig and ITIM domains
BsAb	bispecific antibody
Nb	nanobody
PD-1	programmed death-1
PD-L1	programmed death-ligand-1
mAbs	monoclonal antibodies
NSCLC	non-small cell lung cancer
ATCC	American Type Culture Collection
ECD	ectodomain
PBLs	peripheral blood lymphocytes
VHH	variable domains of the heavy-chain antibodies

PE-ELISA	periplasmic extract ELISA
BLI	biofilm interferometry
KD	equilibrium dissociation constant
BSA	bovine serum albumin
PBMCs	human peripheral blood mononuclear cells
SEB	staphylococcal enterotoxin B
TGI	index of tumor volume inhibition
HCS	heavy chains
LCs	light chains
FACS	flow cytometry
IC ₅₀	50% inhibitory concentration
EC ₅₀	50% effective concentration

cancer (NSCLC), which showed clinically meaningful improvements in combination cohorts compared with placebo plus atezolizumab [15].

Compared to the combination therapy using two different mAbs, bispecific antibodies (BsAbs) targeting two different antigens have several significant advantages including higher binding specificity, reducing development and therapeutic cost, and obligate effects [16,17]. Here we developed a BsAb targeting TIGIT and PD-L1 using our nanobody (Nb) screening technology. The BsAb showed a synergistic effect on T cell activation compared to monotherapy with anti-TIGIT Nb or anti-PD-L1 Nb.

2. Material and methods

2.1. Cell lines

HEK-293F, MC38, A375 and HEK 293T cells were obtained from the American Type Culture Collection (ATCC). GS-J2/PD-1 and GS-C2/PD-L1 were obtained from Genscript company, China. HEK-293F cells were cultured in FreeStyle™ 293 medium (Invitrogen, Carlsbad, CA, USA), supplemented with 1% Penicillin-Streptomycin (10,000 U/mL) (Invitrogen). MC38, A375 and HEK 293T cells were grown in DMEM (Invitrogen) containing 1% Penicillin-Streptomycin and 10% FBS (Gibco, GrandIsland, NY, USA). GS-J2/PD-1 and GS-C2/PD-L1 cells were grown in F12K complete medium (Invitrogen) containing 1% Penicillin-Streptomycin and 10% FBS.

2.2. PD-L1 Nb and TIGIT Nb library construction and Nb selection

PD-L1 ectodomain (ECD) or TIGIT (ECD) sequence were amplified and inserted into pFUSE-hIgG1-Fc vector (Invivogen, San Diego, CA, USA). These two antigens were expressed in HEK-293F cells and purified with protein A affinity chromatography. Two young healthy male Bactrian camel were immunized with PD-L1(ECD)-Fc or TIGIT (ECD)-Fc mixed with Freund's adjuvant (Sigma-Aldrich, StLouis, MO, USA) once a week. After the seventh immunization, peripheral blood lymphocytes (PBLs) were collected and the phage display libraries containing genes coding variable domains of the heavy-chain antibodies (VHH) were generated according to established methods [18,19]. All procedures were conducted according to the National Institutes of Health guide for the care and use of Laboratory animals.

Nbs specific binding to human PD-L1 or TIGIT were screened through phage display and periplasmic extract ELISA (PE-ELISA), according to previously described procedure [18,20]. After sequencing the selected clones, the VHH fragments were amplified and subcloned into pFUSE-hIgG4-Fc2 vector (Invivogen). The recombinant vector was transfected into HEK-293F cells, and Nb-Fc

proteins were purified by protein A affinity chromatography. Furthermore, the functional Nb-Fc proteins were further selected with blocking activity assay.

2.3. Production of tetravalent PD-L1 Nb-Fc, tetravalent TIGIT NbA-NbB-Fc and multivalent PD-L1/TIGIT BsAb

Tetravalent PD-L1 Nb-Fc consists of 4 PD-L1 Nbs and an IgG4. Tetravalent TIGIT NbA-NbB-Fc consists of 4 TIGIT Nbs with two different antigen recognizing epitopes and an IgG4, while multivalent PD-L1/TIGIT BsAb consists of tetravalent PD-L1 Nb-Fc and tetravalent TIGIT NbA-NbB. The recombinant antibody sequence was amplified and cloned into pcDNA3.1+ vector. The recombinant vectors were transfected into HEK-293F cells, and the Abs were purified by protein A affinity chromatography.

2.4. Preparation of Tecentriq analog and tiragolumab analog

For preparation of positive control antibodies including Tecentriq (atezolizumab, anti-PDL1 mAb) analog and tiragolumab (anti-TIGIT mAb) analog, the DNA sequences of their heavy chains and light chains were synthesized and cloned into pcDNA3.1+ vector respectively. The recombinant vectors were transfected into HEK-293F cells simultaneously, and the antibodies were purified.

2.5. Blocking activity assay

PD-L1/A375 and TIGIT/293T stable cells lines were constructed using a lentiviral packaging system. To determine the activity of anti-PD-L1 Nb-Fc or anti-TIGIT Nb-Fc blocking PD-L1 or TIGIT on the surface of cells, PD-L1/A375 cells and TIGIT/293T cells were incubated with the purified PD-1 (ECD)-Fc or CD155 (ECD)-Fc labeled with biotin respectively, and a gradient concentration of anti-PD-L1 or anti-TIGIT Abs, followed by staining with streptavidin-PE (eBioscience, San Diego, CA, USA). The signals were detected by BD FACS Calibur instrument (BD Biosciences, Franklin Lakes, New Jersey, USA) and data were analyzed using FlowJo V10 software.

2.6. Affinity determination

The kinetics of Nb-Fc binding to recombinant PD-L1 or TIGIT antigen were performed by biofilm interferometry (BLI) with a ForteBio Octet Red 96 instrument (ForteBio, Menlo Park, CA, USA). Briefly, the diluted Nb-Fc, Tecentriq analog or tiragolumab analog (5 µg/mL) were coupled to protein A sensors and then incubated with a series diluted PD-L1 (ECD) or TIGIT (ECD), followed by dissociation in PBST buffer. The binding curves were fit in 1:1 global

fitting mode by Octet analyze software. The association rate and dissociation rate were monitored and the equilibrium dissociation constant (KD) was calculated.

2.7. Specificity analysis

Human PD-L1 (ECD), cynomolgus PD-L1 (ECD), mouse PD-L1 (ECD), human PD-L2 (ECD), human B7H3 (ECD) and human B7H4 (ECD) were amplified and cloned into pFUSE-hlgG1-Fc vector. These recombinant proteins were expressed and purified in HEK293F cells, and 5 µg/mL proteins were coated onto microtiter plates overnight at 4 °C. After blocked with 1% bovine serum albumin (BSA) at 37 °C for 2 h, 10 µg/mL Nb-Fc labeled with biotin was added and incubated at 37 °C for 1 h. Next, the plates were incubated with streptavidin-HRP for another 1 h. The absorbance at 450 nm was measured on Enspire (PerkinElmer, Waltham, MA, USA) after addition of the TMB substrate and stop reaction buffer (Thermo).

2.8. PD-1/PD-L1 reporter assay

PD-1/PD-L1 reporter gene assay kit was obtained from Genscript company, China. Briefly, PD-L1 Target Cells (GS-C2/PD-L1, aAPC cell) were seeded to 384 wells plates at a density of 1×10^4 cells per well. After 24 h, the culture medium was removed, the diluted anti-PD-L1 antibodies and PD-1 Effector Cells (GS-J2/PD-1, T cell) (1.25×10^4 cells per well) were added and incubated at 37 °C for 6 h. Thereafter, ONE-GloTM Luciferase reagent (Promega, Mullion, WI, USA) was added and the firefly luminescence was measured after 10 min on BioTek plate reader (Biotek, Vermont, USA).

2.9. Human IL-2 release assay

Human peripheral blood mononuclear cells (PBMCs) were isolated from fresh blood using Ficoll-Paque Plus (GE Healthcare). 1×10^5 PBMCs/well cultured in RPMI 1640 were stimulated with 4 µg antibodies at 37 °C for 30 min, and further incubated with 0.1 µg/mL or 1 µg/mL staphylococcal enterotoxin B (SEB) (Toxin Technology, Madison, WI). Human IL-2 production in culture supernatant was analyzed at 72 h post stimulation via ELISA kit (R&D Systems).

2.10. Xenograft models

To establish the human colon cancer model, 24 female B-hPD-L1 mice (six-eight weeks old) provided by Beijing Biocytogen Co., Ltd., China were subcutaneously injected with 2×10^6 MC38 cells, resuspended in 0.1 mL PBS mixed with Matrigel Matrix (Corning) with a ratio of 1:1. When tumor volumes reached 100 mm³, the mice were randomly into three groups: PBS as a negative control, 10 mg/kg Tecentriq analog as a positive control, 10 mg/kg Nb-Fc as the experimental groups. Antibodies were given by intraperitoneal injection for 3 days a time and a total of 6 times.

Perpendicular dimensions were measured twice per week after grouping, and the tumor volumes were determined according to the following equation: Tumor volume (mm³) = $1/2 \times (\text{length}) \times (\text{width})^2$. After 20 days, the mice were sacrificed, then the tumors were dissected and photographed.

All mice experiments were performed according to the standard operating procedures approved by the Animal Ethics Committee of Shanghai University of Medicine and Health Sciences.

2.11. Statistical analysis

Statistical analyses were performed using Graphpad Prism 6 software. Data are expressed as mean ± SD or mean ± SEM. The

statistically significant differences were performed by one-way or two-way ANOVA with Holm-Sidak multiple comparisons test. $P < 0.05$ was considered to be significant.

3. Results

3.1. Generation of tetravalent PD-L1 Nb-Fc with high blocking activity, specificity and affinity

Anti-PD-L1 Nbs with specificity were screened and selected from the established anti-PD-L1 Nb phage display library through phage display technology and PE-ELISA (data not shown). One eukaryotic-expressed and humanized protein PD-L1 Nb-Fc was further selected with the highest blocking activity assay by flow cytometry. As indicated in Fig. 1A, PD-L1 Nb-Fc significantly blocked the PD-1/PD-L1 interaction in a dose dependent manner, with higher inhibitory effect than Tecentriq analog, a known PD-L1 function-blocking mAb. To obtain an agent with better clinical therapeutic potential, the PD-L1 Nb was formed into tetravalent Nbs to enhance its antigen affinity. The results showed that tetravalent PD-L1 Nb-Fc exhibited higher blocking activity than PD-L1 Nb-Fc and Tecentriq analog. (IC₅₀: 0.26 µg/mL vs 0.39 µg/mL vs 0.41 µg/mL) (Fig. 1B, Table 1).

We next determined other characterization of tetravalent PD-L1 Nb-Fc including affinity and specificity. The result indicated that the KD value of tetravalent PD-L1 Nb-Fc was similar with that of Tecentriq analog (2.69E-08 M vs 1.21E-08 M) (Fig. 1C, Table 1). The ELISA assay demonstrated that tetravalent PD-L1 Nb-Fc specifically bound to human PD-L1 and cynomolgus PD-L1, but not to mouse PD-L1. Moreover, tetravalent PD-L1 Nb-Fc did not bind to other B7 family members including human PD-L2, human B7H3 and human B7H4 (Fig. 1D). These findings suggest that tetravalent PD-L1 Nb-Fc exhibits high affinity and specificity.

3.2. Tetravalent PD-L1 Nb-Fc blocks the PD-1/PD-L1-mediated biological function

To determine effects of the tetravalent PD-L1 Nb-Fc on the PD-1/PD-L1-mediated biological function, we firstly performed the PD-1/PD-L1 blockade bioassay using cell-based reporter gene system. The results showed that tetravalent PD-L1 Nb-Fc exhibited better blockade effect and T cell activation effect than Tecentriq analog, with 0.66 µg/mL and 0.92 µg/mL of EC₅₀ respectively (Fig. 2A, Table 1). Similarly, tetravalent PD-L1 Nb-Fc significantly induce the release of hIL-2 from two donors compared with IgG4, with the presence of 0.1 µg/mL SEB or 1 µg/mL SEB. Moreover, PBMC stimulation in the group treated with tetravalent PD-L1 Nb-Fc was greater than that treated with Tecentriq analog (Fig. 2B). Taken together, these results imply that tetravalent PD-L1 Nb-Fc exhibits better immune stimulating effect than Tecentriq analog.

3.3. Tetravalent PD-L1 Nb-Fc shows high anti-tumor activity in vivo

Next, we evaluated the anti-tumor effect of tetravalent PD-L1 Nb-Fc in MC38 cells xenograft models. The results indicated that MC38 tumor growth was significantly suppressed in mice treated with 10 mg/kg tetravalent PD-L1 Nb-Fc, compared with PBS-treated control mice. Of note, its inhibitory effect on tumor growth was higher than that of 10 mg/kg Tecentriq analog (index of tumor volume inhibition (TGI): 69% vs 34%) (Fig. 3A and B). As shown in Fig. 3A, the tumors in two of tetravalent PD-L1 Nb-Fc treated mice were completely inhibited. These results suggest that tetravalent PD-L1 Nb-Fc is a promising candidate for the treatment of colon cancer.

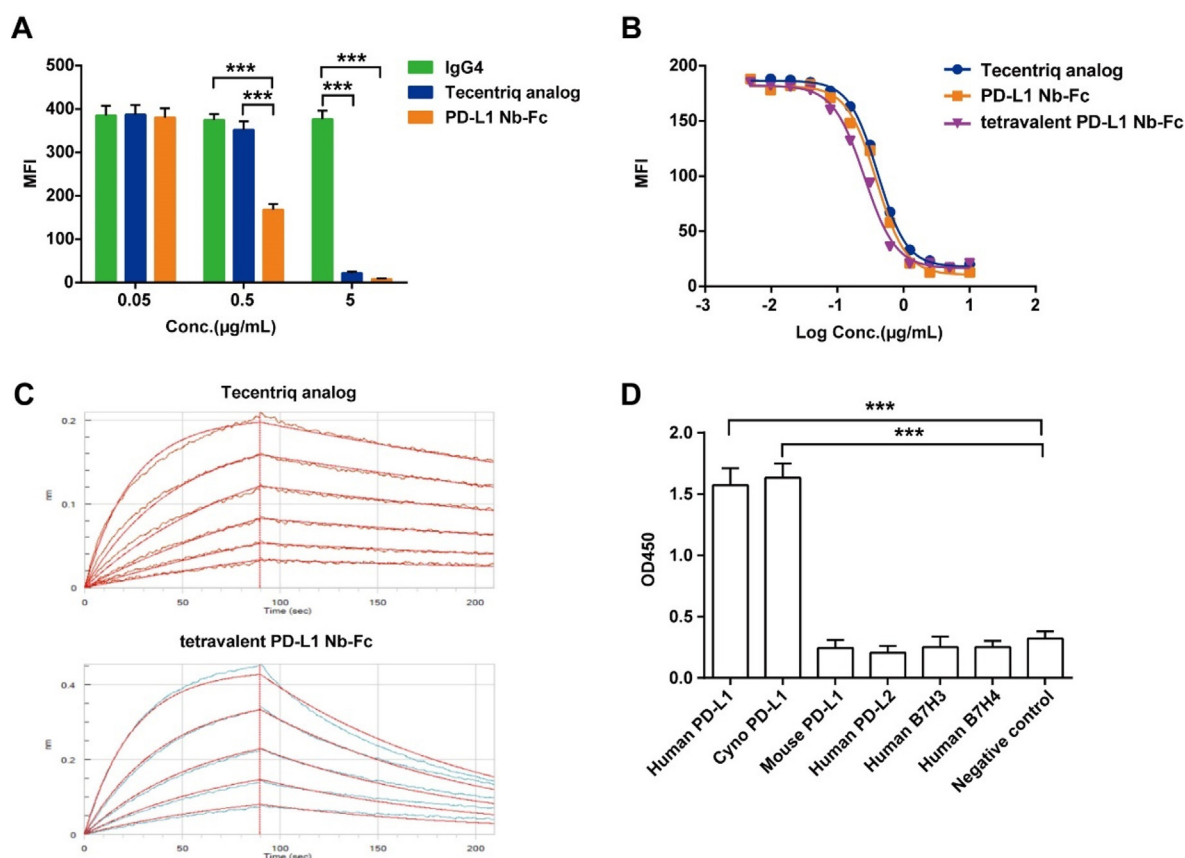


Fig. 1. The blocking activity, affinity and specificity of tetravalent PD-L1 Nb-Fc. (A) The blocking activity of PD-L1 Nb-Fc towards PD-1/PD-L1 interaction was determined by flow cytometry (FACS), with IgG4 and Tecentriq analog as negative and positive control respectively. MFI: median fluorescence intensity. (B) The blocking activities of tetravalent PD-L1 Nb-Fc, PD-L1 Nb-Fc and Tecentriq analog was detected by FACS. (C) The affinity of tetravalent PD-L1 Nb-Fc and Tecentriq analog to PD-L1 was detected by biofilm interferometry (BLI). (D) The specificity of tetravalent PD-L1 Nb-Fc to different antigens was detected by ELISA, with IgG1 as negative control. The data were presented as mean \pm SD. *** $P < 0.001$ versus control.

Table 1

Comparison of blocking effect, affinity and T cell activity among PD-L1 Abs.

	Tecentriq analog	PD-L1 Nb-Fc	Tetravalent PD-L1 Nb-Fc
Blocking effect (IC_{50})	0.41 μ g/mL	0.39 μ g/mL	0.26 μ g/mL
Affinity (KD)	1.21E-08 M	/	2.69E-08 M
PD-1/PD-L1 reporter assay (EC_{50})	0.92 μ g/mL	/	0.66 μ g/mL

^a IC_{50} : 50% inhibitory concentration.

^bKD: equilibrium dissociation constant.

^c EC_{50} : 50% effective concentration.

3.4. Generation of tetravalent TIGIT NbA-NbB with high blocking activity, specificity and affinity

Considering that TIGIT is an inhibitory checkpoint expressed on T cells and NK cells, and plays an important role in the response of antitumor immunity, we screened two TIGIT Nbs (NbA and NbB) from TIGIT Nb phage display library (data not shown). Both of NbA and NbB were humanized and fused to Fc expressed in HEK 293F cells, which were named as TIGIT-NbA-Fc and TIGIT-NbB-Fc. Furthermore, we prepared tetravalent TIGIT NbA-NbB-Fc containing two NbA and two NbB and an IgG4. The results demonstrated that both TIGIT-NbA-Fc and TIGIT-NbB-Fc exhibited higher blocking activity towards TIGIT/CD155 interaction, compared with tiragolumab analog, a known anti-TIGIT mAb. Of note, the tetravalent TIGIT NbA-NbB-Fc exhibited the best blocking activity with EC_{50} of 0.089 μ g/mL (Fig. 4A and Table 2).

Next, in specificity and affinity determination assay, our results indicated that KD value of tetravalent TIGIT NbA-NbB-Fc was similar with tiragolumab analog (1.91E-08 M vs 9.69E-09 M) (Fig. 4B, Table 2). Additionally, tetravalent TIGIT NbA-NbB-Fc was shown to specifically bind human and cynomolgus TIGIT instead of mouse TIGIT (Fig. 4C).

3.5. PD-L1/TIGIT BsAb remains its blocking activity and exhibits higher immune stimulation activity

In order to induce a more powerful antitumor immune effect and facilitate selective binding to tumor cells, we established anti-PD-L1/TIGIT multivalent BsAb. The structure of this multivalent BsAb, which consists of tetravalent PD-L1-Nb-Fc and tetravalent TIGIT NbA-NbB, is illustrated in Fig. 4D. As displayed in Fig. 4E and F, the PD-L1/TIGIT BsAb exhibited the similar PD-1/PD-L1 blocking

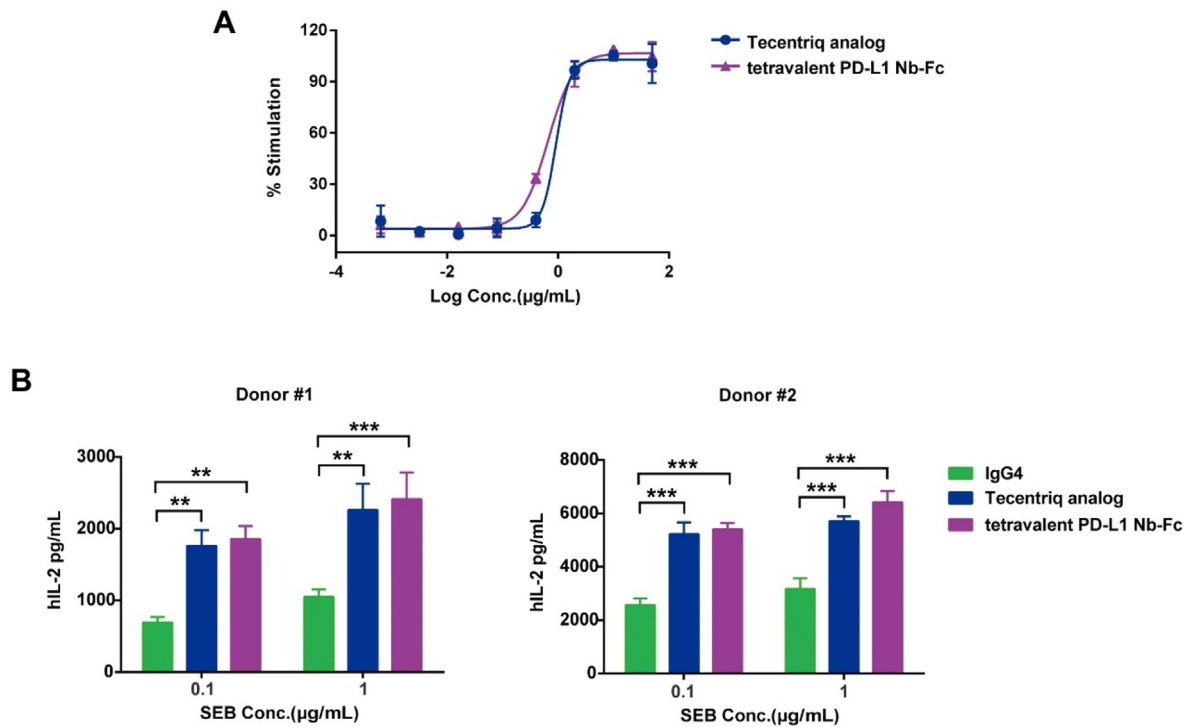


Fig. 2. Effect of tetraivalent PD-L1 Nb-Fc on the biological function mediated by PD-1/PD-L1. (A) T cell activation effect was determined by PD-1/PD-L1 reporter assay. (B) hIL-2 secretion from human PBMCs stimulated by SEB and tetraivalent PD-L1 Nb-Fc was determined by ELISA assay. The PBMCs were derived from two donors. The data were presented as mean \pm SD. The data were presented as mean \pm SD. ** $P < 0.01$, *** $P < 0.001$ versus control.

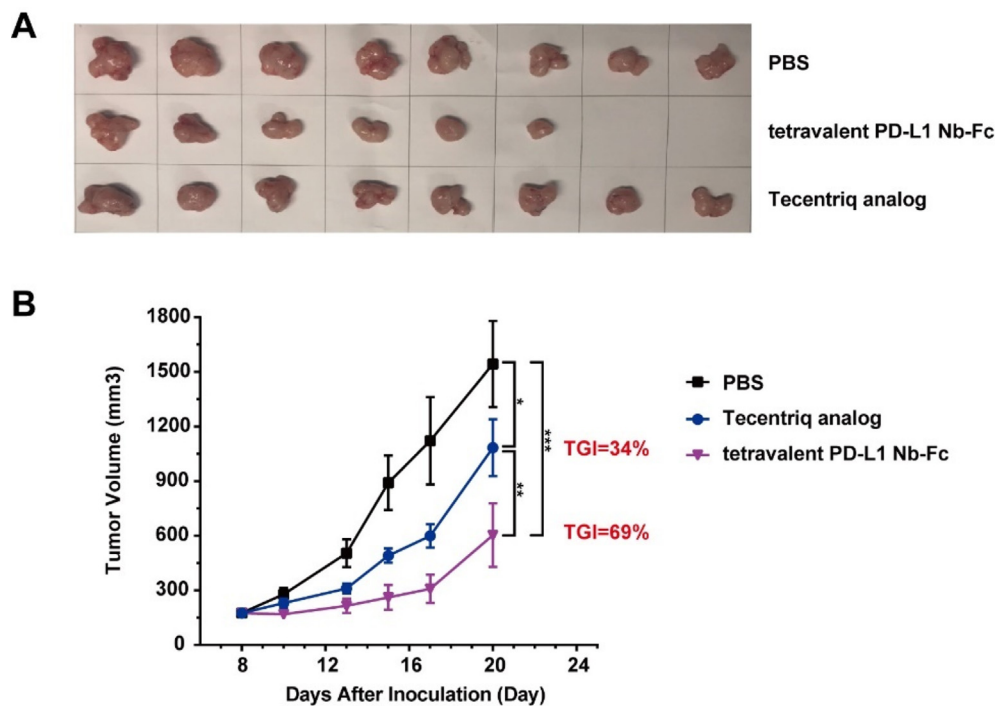


Fig. 3. *In vivo* anti-tumor activities of tetraivalent PD-L1 Nb-Fc in MC38 cells engrafted mice. B-hPD-L1 mice were subcutaneously transplanted with MC38 cells and treated with 10 mg/kg tetraivalent PD-L1 Nb-Fc, 10 mg/kg Tecentriq analog or PBS as control ($n = 8$). (A) Tumor tissues from all mice in each group were shown. (B) The tumor volumes were measured and the index of tumor volume inhibition (TGI) were shown. Each value represents mean \pm SEM. * $P < 0.05$, ** $P < 0.01$, *** $P < 0.001$.

activities to the tetraivalent PD-L1 Nb-Fc (IC_{50} : 0.38 μ g/mL vs 0.25 μ g/mL) (Fig. 4E, Table 3). In parallel with this, the PD-L1/TIGIT BsAb exhibited similar TIGIT/CD155 blocking activities to

tetraivalent TIGIT NbA-NbB-Fc (IC_{50} : 0.15 μ g/mL vs 0.12 μ g/mL) (Fig. 4F, Table 3). In addition, in the biological functional analysis, with the presence of 1 μ g/mL SEB, the PD-L1/TIGIT BsAb treated

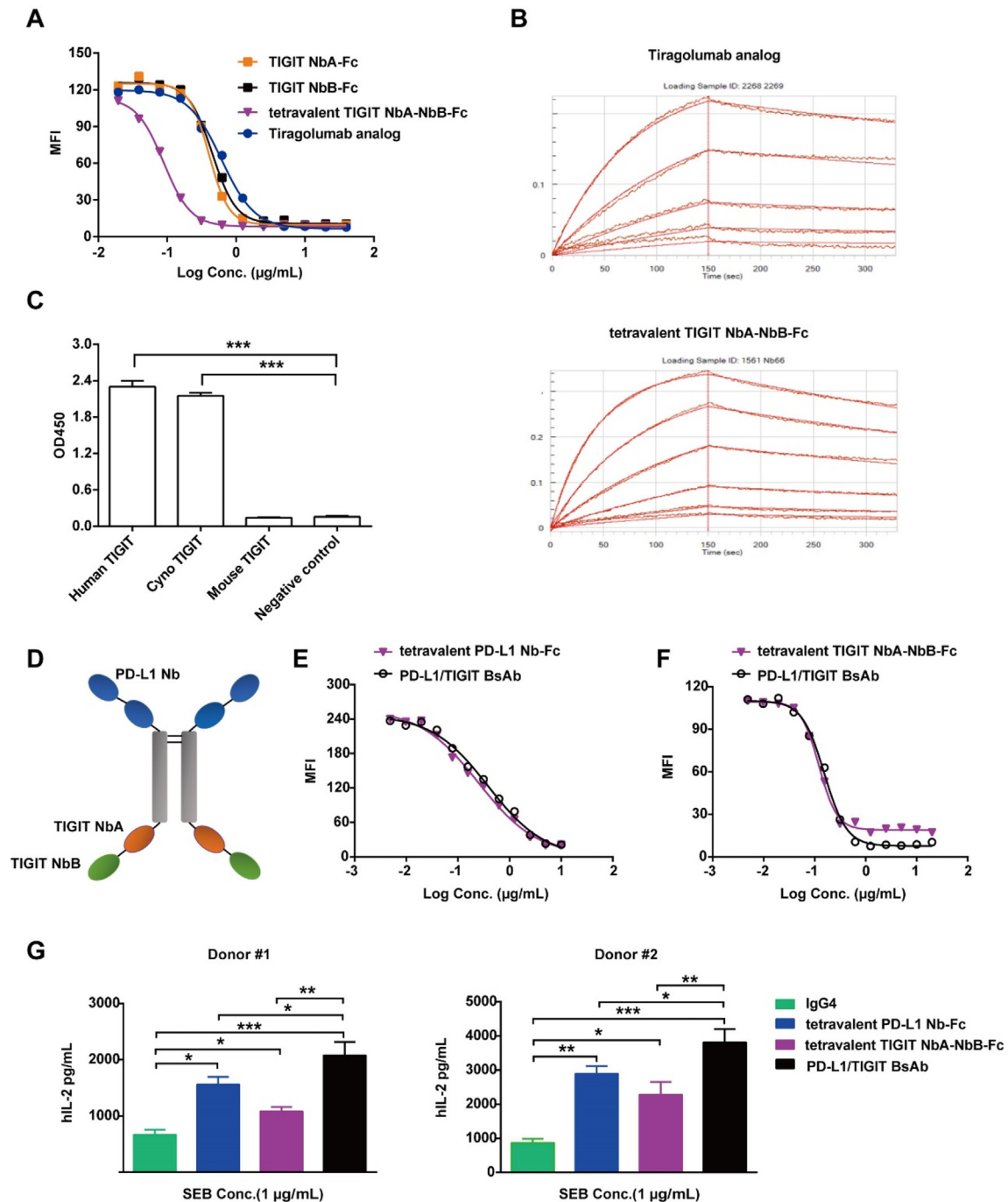


Fig. 4. The characterization of tetravalent TIGIT NbA-NbB-Fc and the functional evaluation of PD-L1/TIGIT BsAb. (A) The blocking activity of TIGIT NbA-NbB-Fc, TIGIT-NbA-Fc and TIGIT-NbB-Fc towards TIGIT/CD155 interaction was determined by FACS, with tiragolumab analog as positive control. (B) The affinity of tetravalent TIGIT NbA-NbB-Fc and tiragolumab analog to TIGIT was detected by BLI. (C) The specificity of tetravalent TIGIT NbA-NbB-Fc to different antigens was detected by ELISA, with IgG1 as negative control. (D) The structure of anti-PD-L1/TIGIT BsAb. (E) The blocking activity of tetravalent PD-L1 Nb-Fc and PD-L1/TIGIT BsAb towards PD-1/PD-L1 interaction was detected by FACS. (F) The blocking activity of tetravalent TIGIT NbA-NbB-Fc and PD-L1/TIGIT BsAb towards TIGIT/CD155 interaction was detected by FACS. (G) hIL-2 secretion from human PBMCs stimulated by SEB and Nb-Fc was determined by ELISA assay. The PBMCs were derived from two donors. The data were presented as mean \pm SD. * $P < 0.05$, ** $P < 0.01$, *** $P < 0.001$.

Table 2
Comparison of blocking effect and affinity among TIGIT Abs.

	tiragolumab analog	TIGIT-NbA-Fc	TIGIT-NbB-Fc	tetravalent TIGIT NbA-NbB-Fc
Blocking effect (IC_{50})	0.615 μ g/mL	0.405 μ g/mL	0.452 μ g/mL	0.089 μ g/mL
Affinity (KD)	9.69E-09 M	/	/	1.91E-08 M

^a IC_{50} : 50% inhibitory concentration.

^bKD: equilibrium dissociation constant.

Table 3

Comparison of blocking effect between tetravalent PD-L1 or TIGIT Nb-Fc and PD-L1/TIGIT BsAb.

	tetravalent PD-L1 Nb-Fc	PD-L1/TIGIT BsAb
PD-1/PD-L1 blocking effect (IC ₅₀)	0.25 µg/mL	0.38 µg/mL
	tetravalent TIGIT NbA-NbB-Fc	PD-L1/TIGIT BsAb
TIGIT/CD155 blocking effect (IC ₅₀)	0.12 µg/mL	0.15 µg/mL

IC₅₀: 50% inhibitory concentration.

group demonstrated the significantly increased hIL-2 secretion, compared to the tetravalent PD-L1 Nb-Fc treated group ($P < 0.05$) and tetravalent TIGIT NbA-NbB-Fc treated group ($P < 0.01$) (Fig. 4G). These results suggest that the multivalent BsAb co-targeting PD-L1 and TIGIT synergistically enhanced T cell activities, compared to the single treatment of PD-L1 Nbs or TIGIT Nbs.

4. Discussion

The use of the immune system to treat malignant tumors is considered to be the most promising treatment strategy, which can produce a deep and durable response to a variety of tumors, making people see the hope of curing tumors [21,22]. With the widespread use of mAbs targeting PD-1/PD-L1 in clinical practice, a large number of patients have been found to fail to respond or developed resistance after response [23,24]. In the recent clinical and pre-clinical studies, anti-PD-1/PD-L1 mAbs, combined with other checkpoint antagonists (e.g. CTLA-4, LAG-3), demonstrated cumulative or synergistic antitumor immune effects [3,25], which provides a new treatment option for tumor patients resistant to or having no response to the treatment of PD-1/PD-L1 blockade. In this study, we developed a novel bispecific antibody with dual-blockade activities of PD-L1 and TIGIT, which can synergistically enhance the function of activating T cells *in vitro*.

BsAbs have become one of the most attractive areas for drug development in recent years, with more than 85 BsAbs in clinical development [26]. Now, dozens of different technology platforms represented by Duobody, DVD-Ig, DART and BiTE are available for BsAbs development. However, there is still much room for improvement in the production and purification of BsAbs due to the highly heterogeneous pairing of heavy chains (HCs) and light chains (LCs) [27,28].

In this study, we used Nbs as the modules to construct BsAbs. Nb, a single-domain antibody derived from camel heavy chain antibodies, is characterized by small size, high stability and high affinity [29]. Thus, BsAbs based-on Nbs can avoid the heterogeneous pairing of HCs and LCs, resulting in the improvement of product quality and productivity of BsAbs by simplifying the separation and purification steps.

To obtain functional BsAbs, each antigen-binding domain of BsAbs needs to bind the antigens with high affinity and specificity. In our study, the tetravalent PD-L1 Nb-Fc was shown to specifically bind to human and monkey PD-L1, but not to other species of PD-L1. Moreover, the tetravalent PD-L1 Nb-Fc effectively enhanced T cell function *in vitro* and inhibited tumor growth *in vivo*. Similarly, TIGIT-targeted Nb-Fc specifically bound to human and monkey TIGIT, but not to other species of TIGIT. Moreover, the tetravalent TIGIT Nb-Fc effectively enhanced T cell function. Based on these findings, we constructed a multivalent BsAb targeting PD-L1 and TIGIT, which maintained the binding affinity of the parental Nbs to the antigen. This BsAb synergistically enhanced T cell activities *in vitro*. These findings indicate that we have obtained a novel BsAb that can functionally block PD-L1 and TIGIT. It is worthy to study the anti-tumor activities of this BsAb *in vivo*.

Declaration of competing interest

None.

Acknowledgements

This study was sponsored by the National Natural Science Foundation of China (81673344, 81902052) and Shanghai Sailing Program (20YF1434300).

References

- [1] S.T. Kim, R. Cristescu, A.J. Bass, K.-M. Kim, J.I. Odegaard, K. Kim, X.Q. Liu, X. Sher, H. Jung, M. Lee, Comprehensive molecular characterization of clinical responses to PD-1 inhibition in metastatic gastric cancer, *Nat. Med.* 24 (2018) 1449–1458.
- [2] O. Milberg, C. Gong, M. Jafarnejad, I.H. Bartelink, B. Wang, P. Vicini, R. Narwal, L. Roskos, A.S. Popel, A QSP model for predicting clinical responses to monotherapy, combination and sequential therapy following CTLA-4, PD-1, and PD-L1 checkpoint blockade, *Sci. Rep.* 9 (2019) 1–17.
- [3] A. Rotte, Combination of CTLA-4 and PD-1 blockers for treatment of cancer, *J. Exp. Clin. Oncol.* 38 (2019) 255.
- [4] R.J. Johnston, L. Comps-Agrar, J. Hackney, X. Yu, M. Huseni, Y. Yang, S. Park, V. Jain, H. Chiu, B. Irving, The immunoreceptor TIGIT regulates antitumor and antiviral CD8+ T cell effector function, *Canc. Cell* 26 (2014) 923–937.
- [5] H. Harjunpää, C. Guillerey, TIGIT as an emerging immune checkpoint, *Clin. Exp. Immunol.* 200 (2020) 108–119.
- [6] N.A. Manieri, E.Y. Chiang, J.L. Grogan, TIGIT: a key inhibitor of the cancer immunity cycle, *Trends Immunol.* 38 (2017) 20–28.
- [7] Y. He, H. Peng, R. Sun, H. Wei, H.-G. Ljunggren, W.M. Yokoyama, Z. Tian, Contribution of inhibitory receptor TIGIT to NK cell education, *J. Autoimmun.* 81 (2017) 1–12.
- [8] L. Wu, L. Mao, J.-F. Liu, L. Chen, G.-T. Yu, L.-L. Yang, H. Wu, L.-L. Bu, A.B. Kulkarni, W.-F. Zhang, Blockade of TIGIT/CD155 signaling reverses T-cell exhaustion and enhances antitumor capability in head and neck squamous cell carcinoma, *Cancer Immunol. Res.* 7 (2019) 1700–1713.
- [9] Q. Zhang, J. Bi, X. Zheng, Y. Chen, H. Wang, W. Wu, Z. Wang, Q. Wu, H. Peng, H. Wei, Blockade of the checkpoint receptor TIGIT prevents NK cell exhaustion and elicits potent anti-tumor immunity, *Nat. Immunol.* 19 (2018) 723–732.
- [10] C. Guillerey, H. Harjunpää, N. Carrié, S. Kassem, T. Teo, K. Miles, S. Krumeich, M. Weulersse, M. Cuisinier, K. Stannard, TIGIT immune checkpoint blockade restores CD8+ T-cell immunity against multiple myeloma, *Blood* 132 (2018) 1689–1694.
- [11] K.O. Dixon, M. Schorer, J. Nevin, Y. Etminan, Z. Amoozgar, T. Kondo, S. Kurtulus, N. Kassam, R.A. Sobel, D. Fukumura, Functional anti-TIGIT antibodies regulate development of autoimmunity and antitumor immunity, *J. Immunol.* 200 (2018) 3000–3007.
- [12] L.E. Lucca, P.-P. Axisa, E.R. Singer, N.M. Nolan, M. Dominguez-Villar, D.A. Hafler, TIGIT signaling restores suppressor function of Th1 Tregs, *JCI Insight* 4 (2019).
- [13] A.L. Hung, R. Maxwell, D. Theodoros, Z. Belcaid, D. Mathios, A.S. Luksik, E. Kim, A. Wu, Y. Xia, T. Garzon-Muvdi, TIGIT and PD-1 dual checkpoint blockade enhances antitumor immunity and survival in GBM, *Oncolimmunology* 7 (2018), e1466769.
- [14] J.-M. Chauvin, O. Pagliano, J. Fourcade, Z. Sun, H. Wang, C. Sander, J.M. Kirkwood, T.-h.T. Chen, M. Maurer, A.J. Korman, TIGIT and PD-1 impair tumor antigen-specific CD8+ T cells in melanoma patients, *J. Clin. Investig.* 125 (2015) 2046–2058.
- [15] D. Rodriguez-Abreu, M.L. Johnson, M.A. Hussein, M. Cobo, A.J. Patel, N.M. Secen, K.H. Lee, B. Massuti, S. Hiret, J.C.-H. Yang, Primary analysis of a randomized, double-blind, phase II study of the anti-TIGIT antibody tiragolumab (tira) plus atezolizumab (atezo) versus placebo plus atezo as first-line (1L) treatment in patients with PD-L1-selected NSCLC (CITYSCAPE), *Am. Soc. Clin. Oncol.* 38 (2020) 9503.
- [16] C. Rader, Bispecific antibodies in cancer immunotherapy, *Curr. Opin. Biotechnol.* 65 (2020) 9–16.
- [17] G. Fan, Z. Wang, M. Hao, J. Li, Bispecific antibodies and their applications, *J. Hematol. Oncol.* 8 (2015) 130.

- [18] M. Zhu, Y. Hu, G. Li, W. Ou, P. Mao, S. Xin, Y. Wan, Combining magnetic nanoparticle with biotinylated nanobodies for rapid and sensitive detection of influenza H3N2, *Nanoscale Res. Lett.* 9 (2014) 528.
- [19] J. Yan, P. Wang, M. Zhu, G. Li, E. Romao, S. Xiong, Y. Wan, Characterization and applications of Nanobodies against human procalcitonin selected from a novel naive Nanobody phage display library, *J. Nanobiotechnol.* 13 (2015) 33.
- [20] M. Zhu, X. Gong, Y. Hu, W. Ou, Y. Wan, Streptavidin-biotin-based directional double Nanobody sandwich ELISA for clinical rapid and sensitive detection of influenza H5N1, *J. Transl. Med.* 12 (2014) 352.
- [21] H.O. Alsaab, S. Sau, R. Alzhrani, K. Tatiparti, K. Bhise, S.K. Kashaw, A.K. Iyer, PD-1 and PD-L1 checkpoint signaling inhibition for cancer immunotherapy: mechanism, combinations, and clinical outcome, *Front. Pharmacol.* 8 (2017) 561.
- [22] L.A. Emens, P.A. Ascierto, P.K. Darcy, S. Demaria, A.M. Eggermont, W.L. Redmond, B. Seliger, F.M. Marincola, Cancer immunotherapy: opportunities and challenges in the rapidly evolving clinical landscape, *Eur. J. Cancer* 81 (2017) 116–129.
- [23] N.L. Syn, M.W. Teng, T.S. Mok, R.A. Soo, De-novo and acquired resistance to immune checkpoint targeting, *Lancet Oncol.* 18 (2017) e731–e741.
- [24] Y. Jiang, M. Chen, H. Nie, Y. Yuan, PD-1 and PD-L1 in cancer immunotherapy: clinical implications and future considerations, *Hum. Vaccines Immunother.* 15 (2019) 1111–1122.
- [25] S.P. Patel, M. Othus, Y.K. Chae, F.J. Giles, D.E. Hansel, P.P. Singh, A. Fontaine, M.H. Shah, A. Kasi, T. Al Baghdadi, A Phase II basket trial of dual anti-CTLA-4 and anti-PD-1 blockade in rare tumors (DART SWOG 1609) in patients with nonpancreatic neuroendocrine tumors, *Clin. Canc. Res.* 26 (2020) 2290–2296.
- [26] A.F. Labrijn, M.L. Janmaat, J.M. Reichert, P.W. Parren, Bispecific antibodies: a mechanistic review of the pipeline, *Nat. Rev. Drug Discov.* 18 (2019) 585–608.
- [27] F.V. Suurs, M.N. Lub-de Hooge, E.G. de Vries, D.J.A. de Groot, A review of bispecific antibodies and antibody constructs in oncology and clinical challenges, *Pharmacol. Ther.* 201 (2019) 103–119.
- [28] Q. Wang, Y. Chen, J. Park, X. Liu, Y. Hu, T. Wang, K. McFarland, M.J. Betenbaugh, Design and production of bispecific antibodies, *Antibodies* 8 (2019) 43.
- [29] P. Bannas, J. Hambach, F. Koch-Nolte, Nanobodies and nanobody-based human heavy chain antibodies as antitumor therapeutics, *Front. Immunol.* 8 (2017) 1603.